An Image-Based Model for Assisting in Diagnosing Malignant Esophageal Lesions During Lugol Chromoendoscopic Examination

Mengfei Liu, PhD[1,*], Zifan Qi, MS[1,*], Ren Zhou, PhD[1,*], Chuanhai Guo, BS[1], Anxiang Liu, MD[2], Haijun Yang, MD[3], Fenglei Li, BS[4], Liping Duan, MD[5], Lin Shen, MD[6], Qi Wu, MD[7], Zhen Liu, PhD[1], Yaqi Pan, MS[1], Fangfang Liu, PhD[1], Ying Liu, PhD[1], Huanyu Chen, BS[1], Zhe Hu, BS[1], Hong Cai, MD[1], Zhonghu He, PhD[8] and Yang Ke, MD[8]

INTRODUCTION: **Image-based diagnostic tools that aid endoscopists to biopsy putative esophageal malignant lesions are essential for ensuring the standardization and quality of Lugol chromoendoscopy. But there is no such model available yet.**

Model for esophageal Lugol-unstained lesions diagnosis

Perspective cohort study

Development set

- ESECC randomized controlled trial (NCT01688908)
- 99 cases out of 1099 participants included

External validation set

- Clinical outpatient cohort from Anyang Cancer Hospital
- 179 cases out of 603 participants included

Data collection

- **Lugol-unstained lesions characteristics:** Size/Irregularity/Border sharpness/Mosaic staining/Dark boundary/Lesion numbers
- **Demographic information:** age, gender, BMI, ESCC family history, etc.

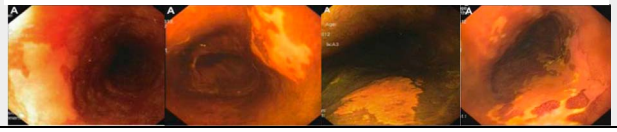

Findings

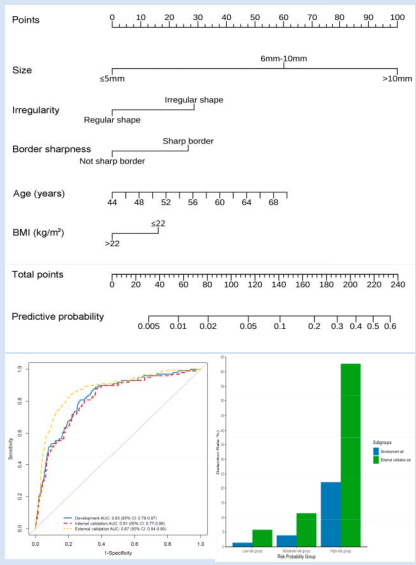

Conclusions

- A model using Lugol-unstained lesion size, irregularity, border sharpness, age, and BMI could assist endoscopists make biopsy decision.
- 81–83% of esophageal high-grade intraepithelial neoplasia and above cases could be effectively enriched in high-risk group in both development and external validation set.

Liu, Qi, and Zhou et al. *Clin Trans Gastroenterol.* 2025.
doi:10.14309/ctg.0000000000000835

Clinical and Translational GASTROENTEROLOGY

[1]Key Laboratory of Carcinogenesis and Translational Research (Ministry of Education/Beijing), Department of Genetics, Peking University Cancer Hospital & Institute, Beijing, China; [2]Endoscopy Center, Anyang Cancer Hospital, Anyang, Henan Province, China; [3]Department of Pathology, Anyang Cancer Hospital, Anyang, Henan Province, China; [4]Hua County People's Hospital, Henan Province, China; [5]Department of Gastroenterology, Peking University Third Hospital, Beijing, China; [6]State Key Laboratory of Holistic Integrative Management of Gastrointestinal Cancers, Beijing Key Laboratory of Carcinogenesis and Translational Research, Department of Gastrointestinal Oncology, Peking University Cancer Hospital & Institute, Beijing, China; [7]State Key Laboratory of Holistic Integrative Management of Gastrointestinal Cancers, Beijing Key Laboratory of Carcinogenesis and Translational Research, Endoscopy Center, Peking University Cancer Hospital & Institute, Beijing, China; [8]State Key Laboratory of Molecular Oncology, Beijing Key Laboratory of Carcinogenesis and Translational Research, Department of Genetics, Peking University Cancer Hospital & Institute, Beijing, China. **Correspondence:** Yang Ke, MD. E-mail: keyang@bjmu.edu.cn. Zhonghu He, PhD. E-mail: zhonghuhe@foxmail.com.
*Mengfei Liu, Zifan Qi, and Ren Zhou contributed equally to this article.
Received August 20, 2024; accepted February 20, 2025; published online March 3, 2025

METHODS: **We developed a diagnostic model using endoscopic Lugol-unstained lesions (LULs) features and baseline data from 1,099 individuals enrolled from a large-scale population-based ESCC screening cohort. Six hundred three participants from a clinical outpatient cohort were included as the external validation set. High-grade intraepithelial neoplasia and above lesions identified at baseline or within 1 year after screening were defined as outcome. The final model was determined using logistic regression analysis by the Akaike information criterion.**

RESULTS: **The optimal diagnostic model contained the size, irregularity, sharp border of LUL, age, and body mass index of the participant, with the area under the curve of 0.83 (95% confidence interval [CI]: 0.78–0.87) in the development set, 0.81 (95% CI: 0.77–0.86) in the internal validation set, and 0.87 (95% CI: 0.84–0.90) in the external set. This model stratified individuals with LULs into low-risk, moderate-risk, and high-risk groups based on tertiles of predicted probabilities. The high-risk group accounted for <40% participants but enriched 80.8% and 82.7% of high-grade intraepithelial neoplasia and above cases in the development and external validation sets, respectively, achieving detection ratios 16.2 and 11.0 times higher than the low-risk group.**

DISCUSSION: **Our model can help maintain consistency and accuracy in detecting esophageal malignancy through Lugol chromoendoscopy, particularly in primary healthcare units in high-risk rural areas.**

KEYWORDS: precision biopsy; risk stratification; esophageal malignant lesions; endoscopic diagnosis; ESECC

SUPPLEMENTARY MATERIAL accompanies this paper at http://links.lww.com/CTG/B287

Clinical and Translational Gastroenterology 2025;16:e00835. https://doi.org/10.14309/ctg.0000000000000835

INTRODUCTION

Esophageal cancer (EC) is one of the most common cancers worldwide, which ranks eleventh and seventh for incidence and mortality (1). Of 511,000 new EC cases and 445,000 deaths in 2022, more than 40% cases and deaths were contributed by China (1,2). Esophageal squamous cell carcinoma (ESCC) is the predominant EC subtype in China and accounts for 85% of EC cases (3,4).

To date, early diagnosis and treatment are recognized as an effective approach for ESCC prevention, and Lugol chromoendoscopy (LCE) is used as the gold standard technique in population-level screening programs (5). LCE is based on the reaction of iodine and intracellular glycogen, in which suspicious lesions become unstained and can be visually distinguished from the surrounding brownish normal esophageal epithelium (6). As LCE has a >95% sensitivity but unsatisfactory specificity in identifying cancerous lesions (7), targeted biopsy and pathologic diagnosis are necessary to further confirm the histologic characteristics of Lugol-unstained lesions (LULs).

According to clinical experiences, a biopsy is recommended for LULs with a diameter ≥5 mm (8–10). However, LULs of diameter >5 mm can be detected among more than 70% of screened subjects in the population-based screening of ESCC (9), and over 95% of these biopsies were diagnosed as nonmalignant lesions. On the other hand, nearly 45% of incident ESCC cases during a median follow-up of 4.2 years after screening were reported as nondysplasia at index endoscopy (11), indicating the existence of inadequate biopsy, missed diagnosis, and insufficient surveillance in screening practice. Moreover, high-risk areas for ESCC mainly resident in underdeveloped regions, where the screening is performed by junior endoscopists in primary care units, with large variations in technical proficiency. Various factors, including the limited clinical experience and the preference for minimizing the risk brought by tissue biopsy, contribute to an overlooked malignant lesion during the screening process. A quantitative and endoscopic image-based tool for auxiliary diagnosis is urgently warranted, to establish a more standardized and precise targeted biopsy during LCE screening, as compared with the current experience-based judgment of the endoscopist alone.

Endoscopic features, such as the size of LULs and the sharpness of LULs border, etc., have been reported to be indicative of the malignancy of esophageal lesions (12–15). However, no quantitative diagnostic model based on endoscopic features of LULs has been developed to assist endoscopists in the biopsy decision under LCE in real time for population-level ESCC screening.

The aim of this study was to develop an easy-to-use diagnostic model mainly using endoscopic features of LULs as predictors to promote the risk-based precision biopsy in the screening of ESCC, based on a large-scale population-level ESCC screening cohort, and externally validated by a clinical outpatient cohort.

METHODS

Study population

Development set. Subjects of the development set were enrolled from the screening arm of the Endoscopic Screening for Esophageal Cancer in China (ESECC trial, NCT01688908) (16). The ESECC trial was initiated in 2012, and 668 villages in Hua County, Anyang, Henan Province, a high-risk region for ESCC in China, were randomly selected and allocated to the screening arm or the control arm at a ratio of 1:1 using blocked randomization based on the population size (16). The inclusion criteria of the ESECC trial can be found elsewhere (16).

A total of 1,204 subjects with abnormalities under white light or LCE out of 15,299 participants from the screening arm were biopsied by the endoscopist in the baseline screening and were

included in this study. We further excluded 105 of them based on the criteria below: (i) endoscopic images regarding the biopsied LULs were unsatisfactory for image review, (ii) advanced ESCC that can be easily determined under white light, and (iii) the questionnaire data were missing. Finally, 1,099 subjects were eligible and analyzed for this study.

External validation set. An external data set from an outpatient cohort conducted at the endoscopic clinic of Anyang Cancer Hospital, Henan Province, from 2019 to 2023 was incorporated. Patients aged 45–69 years who underwent upper gastrointestinal endoscopic examinations during this period were enrolled. The exclusion criteria of this study were as follows: (i) patients with a history of upper gastrointestinal treatment before recruitment, (ii) no suspicious lesions biopsied during the examination, (iii) no use of LCE, and (iv) low-quality endoscopic images unsuitable for retrospective review. Two researchers reviewed the endoscopic images retrospectively and extracted LUL features based on the same standard operating procedure as did in the development set. A total of 603 patients were included in the analysis as the external validation data set.

Endoscopic examination and pathologic diagnosis

Participants included in both development and validation set were performed standard upper gastrointestinal endoscopy with Lugol iodine staining. The entire esophagus was carefully examined by experienced endoscopists, and the abnormal areas detected under white light or LCE were biopsied during endoscopic examination (16). Endoscopic images were captured every 5 cm along the entire esophagus, and more pictures were taken for LULs before the biopsy. Two experienced pathologists from the Anyang Cancer Hospital performed the pathologic analysis blinded to endoscopic findings, and the discrepancies in diagnoses were adjudicated by consultation. The histologic grade of specimens was categorized into normal, low-grade intraepithelial neoplasia, high-grade intraepithelial neoplasia (HGIN), and ESCC in development and external validation set. The LUL with the highest pathological diagnosis for those with multiple LULs was used.

Endoscopic image review

Two well-trained researchers retrospectively reviewed the endoscopic images to obtain the features of LULs without knowledge of the pathologic diagnosis (11,17). Six features of unstained areas were recorded, including LUL size (defined as the smaller dimension of diameter or length of a given LUL), mosaic staining, irregularity, border sharpness, dark staining border, and numbers of LULs in the entire esophagus (11,17). A detailed description and standard pictures of these endoscopic features is provided in the Supplementary Digital Content (see Supplementary Material and Supplementary Figures 1–5, http://links.lww.com/CTG/B287).

Questionnaire investigation

Computer-aid one-on-one questionnaire investigation was applied to all individuals before endoscopy (18). Information including demographic factors, lifestyle information, ESCC-related symptoms, and ESCC family history were collected (19).

Outcome definition

The primary outcome in this study was defined as HGIN and above (HGINA) lesions detected at LCE through pathologic analysis, and ESCC cases diagnosed within 1 year after the screening, which were collectively referred to as the prevalent HGINA cases. ESCC cases diagnosed after the screening were identified using the annual follow-up framework of the ESECC trial, which was based on both active door-to-door interviews and passive linkage with local electronic registry approaches to collect incident patients with cancer and all-cause death events. Based on our previous evaluation, the sensitivity of this follow-up strategy for reporting cancers was above 95% (20–22). The outcome in the external validation set was defined as HGINA diagnosed at baseline endoscopy.

Statistical analysis

Model construction. A 2-step process was used to build the diagnosis model. We first used univariate logistic regression analysis to select both the LUL features and questionnaire variables with odds ratio >1.3 and $P < 0.5$. The diagnostic model was built with 3 strategies, after taking into consideration the balance of the simplicity and the performance of models. Strategy I relied solely on the endoscopic features of LULs, whereas strategy II took into account additional factors including age, gender, body mass index (BMI), and family history of ESCC. These factors were easily obtainable before the endoscopic examination. Strategy III included both endoscopic features of LULs and all potential predictors for ESCC, which were gathered through a questionnaire investigation. Then multivariable logistic regression models with backward selection were used on all candidate variables in 3 strategies separately, and the Akaike information criterion was used to determine the final model structure.

Model performance. Receiver operating characteristic curves and the area under curve (AUC) were used to assess the discrimination of a specific model, and the DeLong test was used to compare the difference between models (23,24). All models under 3 strategies were internally validated using leave-one-out cross-validation, and the final selected model underwent external validation (25). A nomogram was established to facilitate the risk assessment when performing endoscopic examinations. To evaluate the final model's risk stratification performance, participants were divided into 3 groups (low-risk, moderate-risk, and high-risk) based on tertiles of predicted probabilities. The detection rate and detection rate ratio in each risk group were calculated.

Statistical analysis was performed using Stata (version 16.1; StataCorp) and R version 4.4.1 (R Foundation for Statistical Computing, Vienna, Austria). All tests were 2-sided and had a significance level of 0.05.

Ethics statement

Research protocols were approved by the Institutional Review Board of the Peking University School of Oncology (approval number: 2011101110, 2018KT111), Beijing, China. All participants provided written informed consent.

RESULTS

Description of the participants in development and validation set

In the development data set, 1,099 participants from the ESECC trial screening arm were included. A total of 99 prevalent HGINA cases were defined, including 4 subjects diagnosed with ESCC within 1 year after screening. For the external validation data set, 603 participants were analyzed, which included 179 detected HGINA cases.

Table 1. Selected characteristics among subjects in the development set and external validation set

Variables	Development set, n (%)	External validation set, n (%)	*P* value
Age			0.009
Median (interquartile range)	61.0 (57.0–65.0)	60.0 (54.0–65.0)	
Gender			0.269
Female	521 (47.4)	269 (44.6)	
Male	578 (52.6)	334 (55.4)	
Body mass index (kg/m^2)			0.010
>22	859 (78.2)	438 (72.6)	
≤22	240 (21.8)	165 (27.4)	
ESCC family history			<0.001
No	939 (85.4)	414 (68.7)	
Yes	160 (14.6)	189 (31.3)	
Pathological diagnosis[a]			<0.001
Non-HGINA	1,000 (91.0)	424 (70.3)	
HGINA	99 (9.0)	179 (29.7)	
Size (mm)			<0.001
≤5	633 (57.6)	349 (57.9)	
6–10	311 (28.3)	124 (20.6)	
>10	155 (14.1)	130 (21.5)	
Irregularity			0.047
No	241 (21.9)	158 (26.2)	
Yes	858 (78.1)	445 (73.8)	
Dark staining border			<0.001
No	743 (67.6)	532 (88.2)	
Yes	356 (32.4)	71 (11.8)	
Sharp border			<0.001
No	439 (39.9)	65 (10.8)	
Yes	660 (60.1)	538 (89.2)	
Mosaic staining			0.695
No	376 (34.2)	212 (35.2)	
Yes	723 (65.8)	391 (64.8)	

ESCC, esophageal squamous cell carcinoma; HGINA, high-grade intraepithelial neoplasia and above.
[a]Among the 99 HGINA cases included, 4 were diagnosed as ESCC within 1 year after screening in the development set.

Compared with the development set, individuals in external validation set were younger, having lower BMI (≤22 kg/m^2), more EC family history, and with higher detection rate of esophageal malignancies. For LUL features, lesions in the external validation set were larger, with more regular shape, and having less dark but sharper border (Table 1). The comparison of demographic and life-style information as well as LUL features between prevalent HGINA cases and noncases of the development set were descripted in Supplementary Digital Content (see Supplementary Table 1, http://links.lww.com/CTG/B287).

Structure of the model

Potential risk factors for the presence of HGINA lesions in this study included specific features of LULs (larger size, mosaic staining, irregular shape, sharp border, and multiple LULs) and certain variables collected during baseline investigation (older age, family history of ESCC, BMI ≤22 kg/m^2, use coal or wood as main cooking fuel, high food temperature, eating rapidly, and ingestion of leftovers).

As presented in Table 2 and Supplementary Digital Content (see Supplementary Figure 6, http://links.lww.com/CTG/B287), the endoscopic model under strategy I finally consisted of the size, irregularity, and sharp border of LUL with an AUC of 0.81 (95% confidence interval [CI]: 0.77–0.86) in the development set and 0.76 (95% CI: 0.71–0.81) in the internal validation. The model under strategy II consisted of the size, irregularity, and sharp border of LUL as well as the age and BMI with an AUC of 0.83 (95% CI: 0.78–0.87) in the development set and 0.81 (95% CI: 0.77–0.86) in internal validation.

Table 2. Development of diagnostic models using endoscopic features of LULs based on 3 strategies

Variables	Multivariable coefficients (95% CI)		
	Strategy 1[a]	Strategy 2[b]	Strategy 3[c]
Size (mm)			
≤5	Ref	Ref	Ref
6–10	1.7 (1.1 to 2.4)	1.7 (1.1 to 2.4)	1.7 (1.1 to 2.4)
>10	2.9 (2.3 to 3.6)	2.8 (2.2 to 3.5)	2.8 (2.2 to 3.5)
Irregularity			
No	Ref	Ref	Ref
Yes	0.8 (0.0 to 1.8)	0.8 (0.0 to 1.8)	0.8 (0.0 to 1.8)
Sharp border			
No	Ref	Ref	Ref
Yes	0.8 (0.3 to 1.3)	0.7 (0.3 to 1.2)	0.8 (0.3 to 1.3)
Age (continuous)	NA	0.1 (0.0 to 0.1)	0.1 (0.0 to 0.1)
BMI (kg/m^2)			
>22	NA	Ref	Ref
≤22		0.5 (−0.1 to 1.0)	0.5 (0.0 to 1.0)
Use coal or wood as main cooking fuel			
No	NA	NA	Ref
Yes			0.4 (−0.1 to 0.9)
Eating speed			
Slow	NA	NA	Ref
Fast			0.8 (0.0 to 1.6)
Ingestion of leftovers			
≤1 time per wk	NA	NA	Ref
>1 time per wk			0.4 (−0.1 to 0.8)
Intercept	−4.9 (−6.0 to −4.0)	−9.1 (−12.4 to −6.1)	−9.7 (−13.1 to −6.5)

BMI, body mass index; CI, confidence interval; LULs, Lugol-unstained lesions; NA, not applicable.
[a]Strategy 1: The multivariable logistic model was conducted based on only features of LULs in a backward selection process according to the Akaike information criterion (AIC).
[b]Strategy 2: The multivariable logistic model was conducted based on features of LULs and easy-to-collect demographic information during endoscopic examination, including age, gender, BMI, and ESCC family history. Backward variable selection using AIC was applied to determine the model structure.
[c]Strategy 3: All variables were first evaluated in univariate logistic regression models, and variables with either $P < 0.05$ or $P < 0.5$ and odds ratio >1.3 were subjected to multivariable logistic regressions, in which the backward AIC was used to determine the final predictor pattern.

The model under strategy III additionally included using coal or wood as the main cooking fuel, eating rapidly, and ingestion of leftovers based on the model under strategy II with an AUC of 0.84 (95% CI: 0.79–0.88) in the development set and 0.82 (95% CI: 0.77–0.86) in internal validation set.

After weighing the model performance and the convenience in application, we recommended model II as final diagnostic model, and this model showed an AUC of 0.87 (95% CI: 0.84–0.90) in the external set (Figure 1). A nomogram to facilitate the assessment of the probability of being HGINA when an LUL is detected in a given individual was also provided to facilitate the application of our model by the endoscopist (Figure 2).

Performance of the model

To evaluate the HGINA enrichment ability of the diagnostic model, subjects were divided into 3 groups based on tertiles of predicted probabilities of the development set (Figure 3). Participants were then further categorized into low-risk, moderate-risk, and high-risk groups based on tertiles of predicted probabilities of the development set, accounting for 5.1%, 14.1%, and 80.8% of all HGINA cases, respectively. This stratification resulted in detection ratios 2.8 and 16.2 times higher for the moderate-risk and high-risk groups compared with the low-risk group in the development set (Table 3). In the external validation set, low-risk, moderate-risk, and high-risk groups contributed 6.1%, 11.2%, and 82.7% HGINA cases, achieving detection ratios 11.0 and 2.0 times higher than the low-risk group for the high-risk and moderate-risk groups, showing a stable discrimination capability of malignant lesions. Assuming the application of this diagnostic model in population-based ESCC screening, the false-positive possibility could be reduced from 91% to 78%.

DISCUSSION

Population-level screening for EC is a massive undertaking (26). In comparison with the traditional universal screening, we have proposed the theoretical framework of precision endoscopic

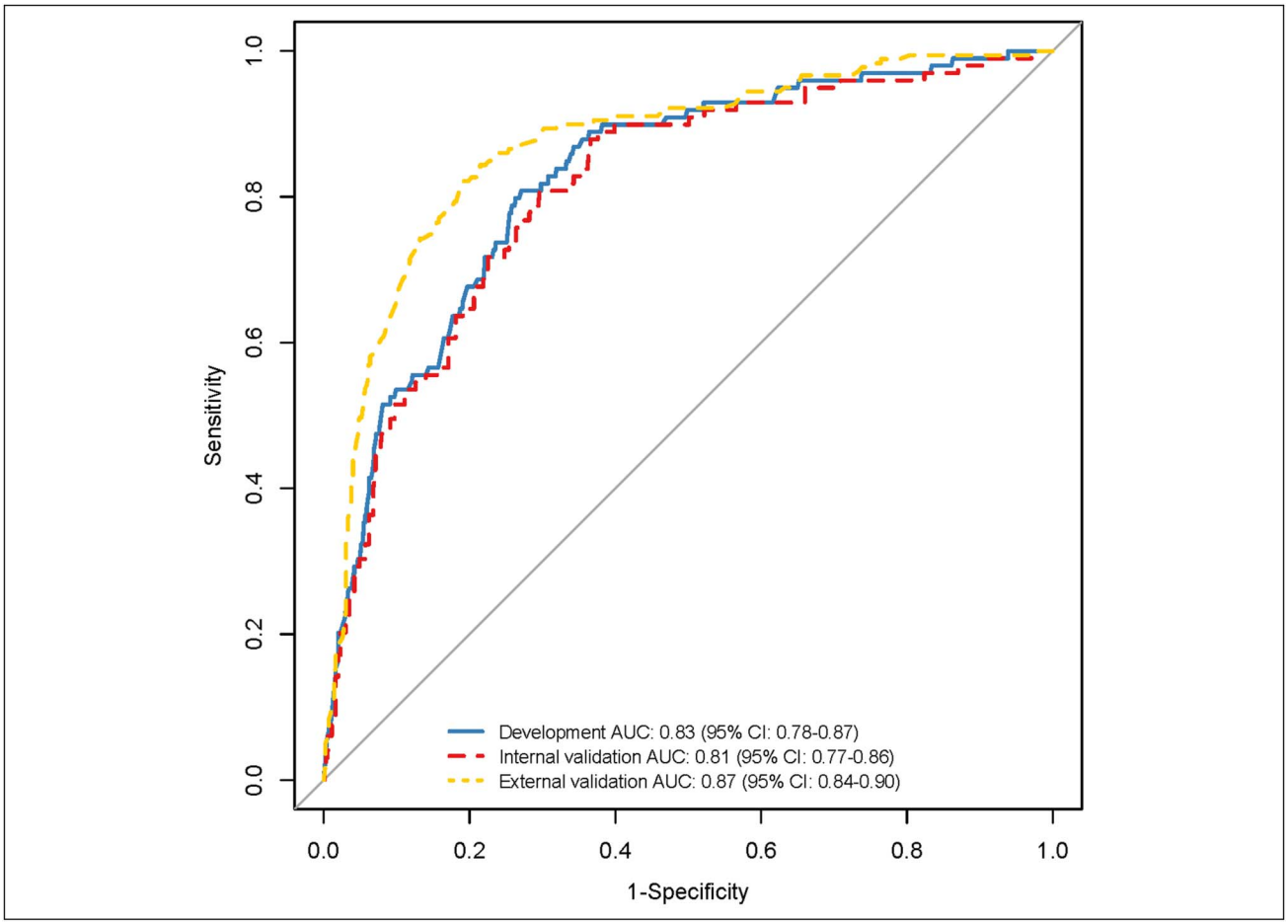

Figure 1. ROC curves of the diagnostic model in the development, internal validation, and external validation sets based on strategy II. AUC, the area under curve; CI, confidence interval; ROC, receiver operating characteristic.

screening for ESCC (27), which aims to improve the cost-effectiveness of screening and reduce potential harm. This goal would be achieved by excluding low-benefit subgroups from the screening process through individualized risk assessments in 3 steps: (i) identification of high-risk individuals as targets for endoscopic screening before examination, (ii) precise identification of malignant lesions for biopsy during endoscopy, and (iii) identification of individuals at high risk of progression as surveillance targets after examination. We have already established the models that identify individuals at high risk in the general population to undergo endoscopic examination before screening (19,28) and the model that predicts the risk of lesion progression for endoscopic surveillance (11) based on baseline screening results of over 15,000 individuals and the longitudinal data from ESECC cohort. However, biopsy-assisted tools for precise biopsy during the endoscopic examination are still lacking (27). This study was the first to develop an image-based diagnostic model under LCE for identifying malignant esophageal lesions, addressing the need for precision biopsy in ESCC screening. The model could aid endoscopists in making accurate biopsy decisions, especially benefiting inexperienced practitioners in primary care units with heavy screening workloads in underdeveloped areas.

The current experts' consensus on ESCC screening in China has emphasized certain indicators for targeted biopsies, such as a high-contrast unstained color in comparison with the surrounding mucosa, well-defined borders, and nonflatness of a given LUL (5). However, endoscopists have faced challenges in prioritizing indicators, leading to inconsistent biopsy criteria, especially for junior endoscopists. To address this, we standardized the contribution of endoscopic and demographic features to malignancy risk for specific LULs in our model.

Our final diagnostic model (model II) consisted of age, BMI, size of LUL, sharpness of the border of LUL, and the irregularity of LUL. Of these selected predictors, age and BMI were well-established ESCC risk factors (16,29). For the selected features, larger size, sharp border, and irregular shape of LUL were predictive for a higher risk of HGINA in this study, which were consistent with results from previous studies and the expert consensus (12–15,17).

We recommended model II as our final diagnostic model for precision biopsy for its simplicity and good performance. It showed ideal discrimination (AUC = 0.83, 95% CI: 0.78–0.87), calibration (Hosmer-Lemeshow test $P = 0.578$, see Supplementary Table 2, http://links.lww.com/CTG/B287), and excellent stability in both internal validation (AUC = 0.81, 95%CI: 0.77–0.86) and external validation (AUC = 0.87, 95% CI: 0.84–0.90). As compared with the model under Strategy II, Model I achieved acceptable discrimination but had insufficient variation in predicting probability and worse internal validation performance compared with Strategy II. Meanwhile, Model III

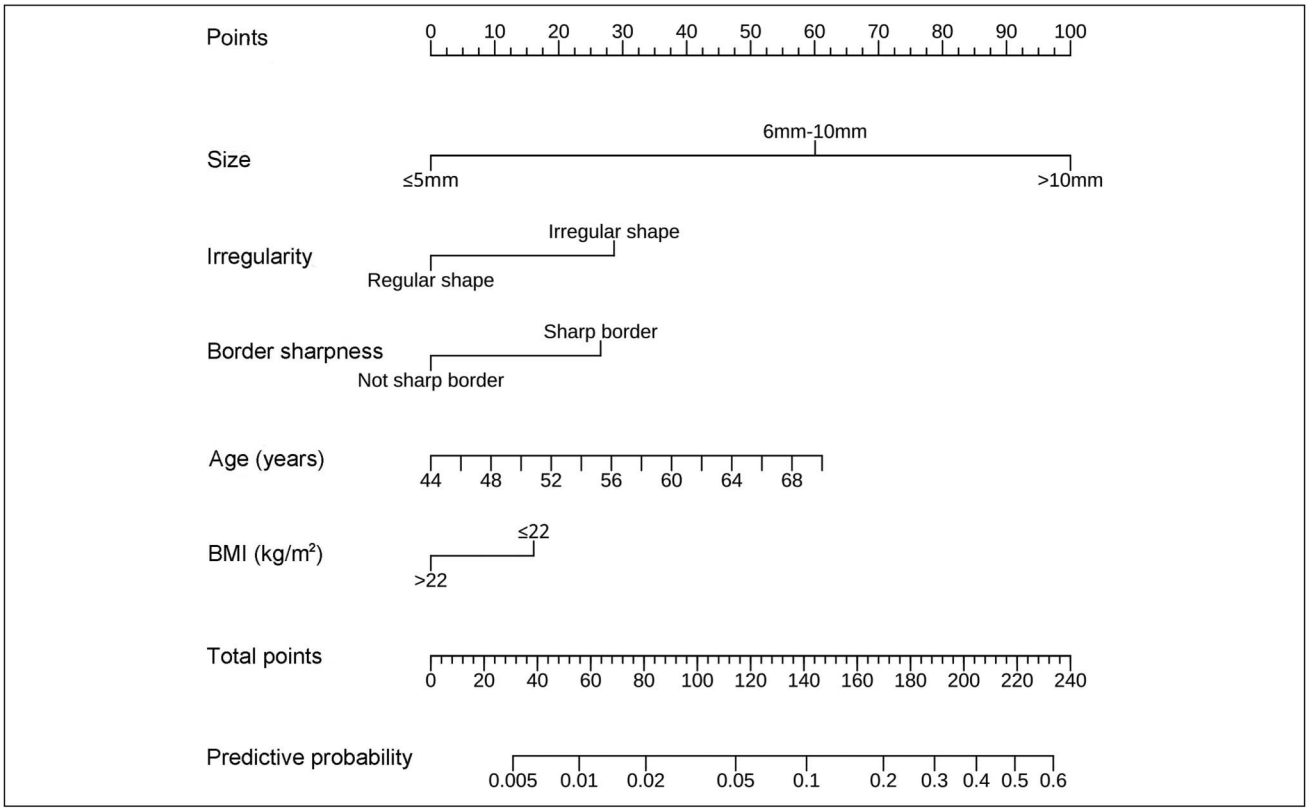

Figure 2. Nomogram of the diagnostic model. BMI, body mass index.

achieved slightly better discrimination performance but increased the workload of collecting epidemiologic information.

Unlike the high detection rate of malignancies among clinic outpatients, ESCC screening targets asymptomatic individuals in high-risk areas, where numerous suspicious lesions often lead to a low absolute detection rate. The current screening practice mainly relies on qualitative and subjective judgment criteria to decide whether to biopsy an LUL, leading to potential malignant LULs being missed. We recommend our quantitative diagnostic tool be applied in settings where the endoscopist has limited experience and heavy workload in ESCC screening because it could assist them in making a more accurate decision for biopsy, which would in turn improve the protection ability of ESCC screening.

This diagnostic tool classifies LCE participants into low-risk, moderate-risk, and high-risk groups based on predicted probabilities. For LULs that were categorized into high-risk group, careful examination and extensively targeted biopsy are recommended because these subjects contributed 80.8% prevalent HGINA cases in the population, with a 16.2-fold detection rate (22.0%) compared with the low-risk group (detection rate: 1.4%).

Biopsies are recommended for the moderate-risk group, accounting for 14.1% of HGINA cases with a 3.8% detection rate. For low-risk LULs, biopsy decisions should rely on clinical judgment because of their low malignancy detection rate but ~5.1% contribution to HGINA cases. The results in external validation set were similar, which validated this recommendation.

Artificial intelligence technology based on graphics has been increasingly applied for auxiliary diagnosis (30–32). It would be helpful to build a diagnostic model-based artificial intelligence assistant that could extract lesion information in real time during endoscopic examinations, automatically calculate the risk of malignant lesions, and display the results on-screen to guide biopsy decisions in clinical workflows in the future.

Although this study was conducted based on a large-scale population-based ESCC screening trial, several limitations should be noted. We extracted the endoscopic features of LULs retrospectively, which might not be so informative compared with real-time judgment when performing LCE.

In summary, we have developed an image-based diagnostic model that combines chromoendoscopic features and simple demographic information to discriminate potential malignant LULs under LCE. This model can assist endoscopists, particularly those who were limited in experience but burdened with extensive screening tasks, in making biopsy decisions during endoscopic examinations. It may help to ensure the standardization and quality of chromoendoscopy in the battlefield of ESCC screening in primary healthcare units in high-risk rural areas. Furthermore, advanced endoscopic techniques such as electronic chromoendoscopy (such as narrow-band imaging) and magnifying endoscopy are gradually being applied more widely to detect and characterize esophageal malignant lesions. Future research into diagnostic models based on these advanced techniques is also warranted to improve the accuracy and efficiency of biopsy in population-level ESCC screening.

CONFLICTS OF INTEREST

Guarantors of the article:Yang Ke, MD & Zhonghu He, PhD.

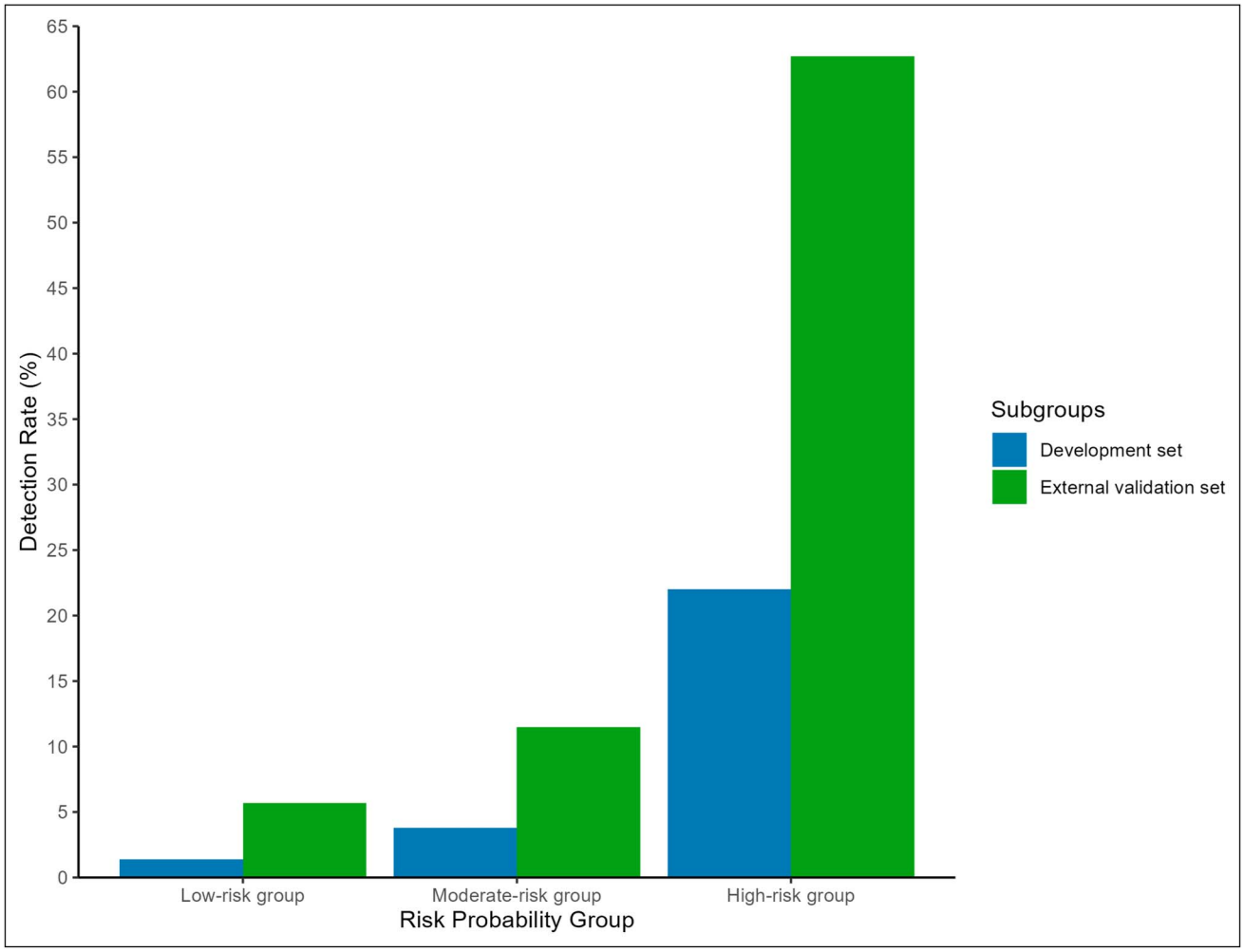

Figure 3. Detection rates of HGINA in 3 groups stratified by predictive risk probabilities based on strategy II in the development and external validation sets. High-risk groups show significantly increased detection rates compared with low-risk groups. The low-risk, moderate-risk, and high-risk groups were defined according to tertiles of predicted probabilities of the development set. HGINA, high-grade intraepithelial neoplasia and above.

Specific author contributions: Y.K., Z.H. and M.L.: study concept and design. Z.H., M.L., Z.L., Z.Q., R.Z., F.L., C.G., F.L., A.L., H.Y., L.S., L.D., Q.W., Y.P., Y.L., H.C., Z.H., and H.C.: acquisition of data. R.Z., Z.Q., M.L., Z.H., and Y.K.: analysis and interpretation of data. R.Z., Z.Q., M.L., Z.H. and Y.K.: drafting of the manuscript. R.Z., Z.Q., and M.L.: statistical analysis. Y.K. and Z.H.: study supervision.

Financial support: This work was supported by the National Key R&D Program of China (grant number 2021YFC2500405), the Beijing Nova Program (grant number Z201100006820093), and the Natural Science Foundation of Beijing Municipality (grant number 7222243).
Potential competing interests: None to report.

Table 3. The enrichment abilities for different types of lesions by diagnostic models using endoscopic features of LULs based on strategy II in the development set and the external validation set

		Development set				External validation set			
Risk stratification[a]	Risk probability range	Non-HGINA cases	HGINA cases	Detection rate (%)	Detection rate ratio (95% CI)	Non-HGINA cases	HGINA cases	Detection rate (%)	Detection rate ratio (95% CI)
Low	0–0.020947436	363	5	1.4	Ref	182	11	5.7	Ref
Moderate	0.020947436–0.083900380	354	14	3.8	2.8 (1.0–7.7)	154	20	11.5	2.0 (1.0–4.1)
High	0.083900380–1	283	80	22.0	16.2 (6.6–39.6)	88	148	62.7	11.0 (6.1–19.7)

CI, confidence interval; HGINA, high-grade intraepithelial neoplasia and above; LULs, Lugol-unstained lesions.
[a]Based on the model-predicted tertiles of malignant lesion probability, subjects were divided into 3 groups, with the predicted probability of esophageal malignancy increasing across low-risk group to high-risk group.

Clinical trial registration: Endoscopic Screening for Esophageal Cancer in China (ESECC) randomized controlled trial (Clinical trial: NCT01688908).

Data availability statement: The data are not available for public access due to the privacy concerns of the participants.

ACKNOWLEDGEMENTS

The authors thank all the following team members and collaborators for their contributions to the field work done for this study, endoscopic examinations and pathologic diagnosis (in alphabetical order by last name and first name): Qiuju Deng, Dong Hang, Fuxiao Li, Shijie Li, Yan Li, Zhihao Lu, Na Shen, Chao Shi, Hongrui Tian, Haixing Wang, Hui Wang, Jing Wang, Minmin Wang, Xicheng Wang, Yan Yan, Wenqing Yuan, Chanyuan Zhang, Xiaotian Zhang and Jun Zhou from Peking University Cancer Hospital & Institute; Kun Wang, Ye Wang and Li Zhang from Peking University Third Hospital; Wanju Gao, Mei Guo, Qianqian Meng, Jun Yang, Liheng Zhang and Lixin Zhang from Anyang Cancer Hospital, Henan Province; Yujie He, Shaojiang Lv and Xiangqin Song from the People's Hospital of Hua County, Henan Province; Xin Yang and Weiguo Xu from the North China University of Science and Technology Affiliated Hospital, Hebei Province; Zengchao Chen from Shandong Qianfoshan Hospital, Shandong Province. The authors would also like to thank the government and the Health and Family Planning Commission of Anyang City and Hua County, Henan Province, all the community leaders, village doctors and participants in the ESECC trial.

Study Highlights

WHAT IS KNOWN

- ✓ Lugol chromoendoscopy is the gold-standard technique for endoscopic screening of esophageal squamous cell carcinoma with high sensitivity but low specificity.
- ✓ There is no image-based diagnostic tool to assist unexperienced endoscopist's decision of taking tissue biopsies when Lugol-unstained lesions are detected.

WHAT IS NEW

- ✓ A model using lesion size, irregularity, border sharpness, age, and body mass index can effectively discriminate the malignant potential of Lugol-unstained lesions in the training and external validation sets.
- ✓ The diagnostic model achieved the area under curve of 0.83 (95% confidence interval: 0.78–0.87) and 0.87 (95% confidence interval: 0.84–0.90) in the development and validation sets.
- ✓ The high-risk group accounted for 80.8% and 82.7% of malignant cases, with a detection ratio 16.2 and 11.0 times higher than that of the low-risk group in the development and external validation sets, respectively.
- ✓ The model could ensure a robust performance of chromoendoscopic screening for esophageal cancer in rural healthcare units.

REFERENCES

1. Bray F, Laversanne M, Sung H, et al. Global cancer statistics 2022: GLOBOCAN estimates of incidence and mortality worldwide for 36 cancers in 185 countries. CA Cancer J Clin 2024;74(3):229–63.
2. Zheng RS, Chen R, Han BF, et al. Cancer incidence and mortality in China, 2022. Zhonghua Zhong Liu Za Zhi 2024;46(3):221–31.
3. Arnold M, Soerjomataram I, Ferlay J, et al. Global incidence of oesophageal cancer by histological subtype in 2012. Gut 2015;64(3):381–7.
4. Chen R, Zheng R, Zhang S, et al. Patterns and trends in esophageal cancer incidence and mortality in China: An analysis based on cancer registry data. J Natl Cancer Cent 2023;3(1):21–7.
5. National Clinical Research Center for Digestive Disease (Shanghai), Chinese Society of Digestive Endoscopy, Digestive Endoscopy Professional Committee of Chinese Endoscopist Association. Chinese expert consensus on diagnosis and treatment of precancerous conditions and lesions of esophageal squamous cell carcinoma. Chin J Dig Endosc 2020;37:853–67.
6. Dawsey SM, Fleischer DE, Wang GQ, et al. Mucosal iodine staining improves endoscopic visualization of squamous dysplasia and squamous cell carcinoma of the esophagus in Linxian, China. Cancer 1998;83(2):220–31.
7. Morita FH, Bernardo WM, Ide E, et al. Narrow band imaging versus Lugol chromoendoscopy to diagnose squamous cell carcinoma of the esophagus: A systematic review and meta-analysis. BMC Cancer 2017; 17(1):54.
8. Carvalho R, Areia M, Brito D, et al. Diagnostic accuracy of Lugol chromoendoscopy in the oesophagus in patients with head and neck cancer. Rev Esp Enferm Dig 2013;105(2):79–83.
9. Wei WQ, Hao CQ, Guan CT, et al. Esophageal histological precursor lesions and subsequent 8.5-year cancer risk in a population-based prospective study in China. Am J Gastroenterol 2020;115(7):1036–44.
10. Yokoyama A, Ohmori T, Makuuchi H, et al. Successful screening for early esophageal cancer in alcoholics using endoscopy and mucosa iodine staining. Cancer 1995;76(6):928–34.
11. Liu M, Liu Z, Liu F, et al. Absence of iodine staining associates with progression of esophageal lesions in a prospective endoscopic surveillance study in China. Clin Gastroenterol Hepatol 2020;18(7):1626–35.e7.
12. Guo Z, Meng L, Tian S, et al. A five-parameter logistic model to predict the possibility of misdiagnosis for improving the specificity of Lugol chromoendoscopy in the diagnosis of esophageal neoplastic lesions. Front Oncol 2021;11:763375.
13. Mori M, Adachi Y, Matsushima T, et al. Lugol staining pattern and histology of esophageal lesions. Am J Gastroenterol 1993;88:701–5.
14. Wang GQ, Wei WQ, Lu N, et al. Significance of screening by iodine staining of endoscopic examination in the area of high incidence of esophageal carcinoma. Chin J Cancer 2003;22(2):175–7.
15. Yokoyama A, Hirota T, Omori T, et al. Development of squamous neoplasia in esophageal iodine-unstained lesions and the alcohol and aldehyde dehydrogenase genotypes of Japanese alcoholic men. Int J Cancer 2012;130(12):2949–60.
16. He Z, Liu Z, Liu M, et al. Efficacy of endoscopic screening for esophageal cancer in China (ESECC): Design and preliminary results of a population-based randomised controlled trial. Gut 2019;68(2):198–206.
17. Liu M, Zhou R, Guo C, et al. Size of Lugol-unstained lesions as a predictor for risk of progression in premalignant lesions of the esophagus. Gastrointest Endosc 2021;93(5):1065–73.e3.
18. Liu F, Guo F, Zhou Y, et al. The Anyang esophageal cancer cohort study: Study design, implementation of fieldwork, and use of computer-aided survey system. PLoS One 2012;7(2):e31602.
19. Liu M, Liu Z, Cai H, et al. A model to identify individuals at high risk for esophageal squamous cell carcinoma and precancerous lesions in regions of high prevalence in China. Clin Gastroenterol Hepatol 2017;15(10): 1538–46.e7.
20. Shi C, Liu M, Liu Z, et al. Using health insurance reimbursement data to identify incident cancer cases. J Clin Epidemiol 2019;114:141–9.
21. Tian H, Xu R, Li F, et al. Identification of cancer patients using claims data from health insurance systems: A real-world comparative study. Chin J Cancer Res 2019;31(4):699–706.
22. Tian H, Yang W, Hu Y, et al. Estimating cancer incidence based on claims data from medical insurance systems in two areas lacking cancer registries in China. EClinicalMedicine 2020;20:100312.
23. DeLong ER, DeLong DM, Clarke-Pearson DL. Comparing the areas under two or more correlated receiver operating characteristic curves: A nonparametric approach. Biometrics 1988;44(3):837–45.
24. Steyerberg EW, Vickers AJ, Cook NR, et al. Assessing the performance of prediction models: A framework for traditional and novel measures. Epidemiology 2010;21(1):128–38.
25. Efron B. Estimating the error rate of a prediction rule–improvement on cross-validation. J Am Stat Assoc 1983;78(382):316–31.

26. He Z, Ke Y. Challenge and future of cancer screening in China: Insights from esophageal cancer screening practice. Chin J Cancer Res 2023;35(6): 584–94.
27. He Z, Ke Y. Precision screening for esophageal squamous cell carcinoma in China. Chin J Cancer Res 2020;32(6):673–82.
28. Liu M, Zhou R, Liu Z, et al. Update and validation of a diagnostic model to identify prevalent malignant lesions in esophagus in general population. EClinicalMedicine 2022;47:101394.
29. Wang SM, Fan JH, Jia MM, et al. Body mass index and long-term risk of death from esophageal squamous cell carcinoma in a Chinese population. Thorac Cancer 2016;7(4):387–92.
30. Furube T, Takeuchi M, Kawakubo H, et al. Automated artificial intelligence-based phase-recognition system for esophageal endoscopic submucosal dissection (with video). Gastrointest Endosc 2024;99(5): 830–8.
31. Yuan L, Yang L, Zhang S, et al. Development of a tongue image-based machine learning tool for the diagnosis of gastric cancer: A prospective multicentre clinical cohort study. EClinicalMedicine 2023;57:101834.
32. Gao Y, Xin L, Feng YD, et al. Feasibility and accuracy of artificial intelligence-assisted sponge cytology for community-based esophageal squamous cell carcinoma screening in China. Am J Gastroenterol 2021; 116(11):2207–15.